IIEEJ Paper

An Accurate and Robust Method for Detecting Fetal Heads in Ultrasound Images Based on Integrating a Voting Scheme and an Improved IRHT

Genta ISHIKAWA†, Rong XU‡, Jun OHYA†, ‡(*Member*), Hiroyasu IWATA†

† Waseda University, Dept. of Modern Mechanical Engineering
‡ Waseda University, Global Information and Telecommunication Institute

<Summary> To achieve accurate and robust detection of fetal heads in US (ultrasound) images, this paper proposes a method that integrates a voting scheme and an improved iterative randomized Hough transform (IRHT) method. First, a skeleton image is extracted from the input US image by pre-processes. Next, the voting scheme, which applies the improved IRHT method to detect ellipses from the skeleton image, is repeated P times, in each of which, if the difference between each detected ellipse's parameter values and each parameter values saved in the list is small, the accumulator of the nearest values in the list is incremented by one (voting); otherwise, the detected *p*arameter values are appended to the list. Finally, the ellipse with the most voted values in the list is outputted as the final detection result. As a result of experiments that use 30 US images captured under different conditions, it turns out that the proposed method achieves a very high ellipse detection rate of 94.97%, which is much higher than IRHT and improved IRHT. In addition, some parameters concerning the proposed method such as the optimal value for P are experimentally explored.

Keywords: fetal head, ultrasound image, ellipse detection, Hough transform, voting

1. Introduction

In recent years, thanks to safety, low cost and noninvasiveness, ultrasound (US) images are frequently applied in prenatal clinic examination for fetal growth evaluation[1], gestational age estimation[2], and fetal weight estimation[3], etc. To evaluate fetal growth, head circumference (HC) is one of the important biometric measurements. However, due to the discontinuity and irregularity of fetal head skulls, low resolution and signal-to-noise ratio of US images, the procedure of fetal head detection could be experience-dependent on and time consuming for medical doctors.

To solve the above-mentioned problem, a number of automatic or semi-automatic methods have been developed for ensuring a better effective, accurate and consistent (not medical-doctor-dependent) HC measurement. Randomized Hough Transform (RHT)[4], Random Sample Consensus (RANSAC)[5], Iterative Randomized Hough Transform (IRHT)[6] are typical techniques for fetal head measurement by ellipse detection, but they may fail when strong noises corrupt the peaks in the parameter spaces, which results in inaccurate measurements. Though some learning based methods[7,8] are proposed to detect fetal heads for a better performance by introducing learning architectures, they often applied IRHT or Hough Transform for ellipse detection and inevitably lead to the same problems of those methods. In addition, the authors have proposed an improved IRHT method[9] for achieving more robust and accurate results by introducing the number (N) of pixels on the ellipse, but it can achieve only unsatisfying detection rates due to noise curves that consist of quite many pixels.

In order to achieve consistent measurements and high detection rates despite the presence of noise curves, we propose an effective voting scheme (known as "bagging"[10]) based on the improved IRHT method[9] for detecting fetal heads in US images contaminated by strong noises. First, pre-processes extract a skeleton image from the input US image. Next, the improved IRHT method detects ellipses from the skeleton image, which is repeated P times. Meanwhile, an ellipse list is created and a voting for each detected result saved in the ellipse list is executed. Finally, the peak (with the most votes) in the ellipse list is outputted as the final detection result.

Section 2 explains the proposed algorithm, section 3 presents experimental results and discussions, section 4 concludes this paper.

2. Algorithm

2.1 Overview

Figure 1 illustrates the proposed method, which exploits a voting scheme based on the improved IRHT[9]. First, a skeleton image is extracted from the input US image by pre-processes (section 2.2). Next, the voting scheme (section 2.4) is carried out as follows. The improved IRHT method is applied to detect ellipses from the skeleton image (section 2.3). This process is repeated *P* times, in each of which, if the difference between each detected ellipse's parameter values and each parameter values saved in the list is small, the accumulator of the nearest values in the list is incremented by one (voting); otherwise, the detected parameter values are appended to the list. Finally, the peak (with the most votes) in the list is outputted as the final ellipse detection result.

2.2 Pre-processes

For detecting the fetal head in the US image, the skeletons of the fetal head skull should be extracted as (a) bright region(s) by pre-processes. Since speckle noise is often superimposed into US images, a bilateral filter[11] with a 5×5 window is utilized to reduce the speckle noise and preserve the edge, where the standard deviations both in the color space and coordinate space are set to 50 in the experiments. Subsequently, a white top-hat transform in mathematical morphology is operated to increase the contrast with an 11×11 window.

After that, the K-means clustering algorithm[12] is applied to distinguish the bright region(s) from the other regions in the fetal US image. The mean value μ_i and the standard deviation σ_i $(i = 1, \ldots, k)$ of cluster (region) i can be calculated from the segmentation results. The class number of K-means is three, because US images of the fetal head are segmented into three components: head skull, soft tissue, and background. Since the K-means method is sensitive to noise, the bright region(s) obtained from the segmentation results could be corrupted by much noise. When we extract the skulls' skeletons as the input to the original or improved IRHT method, we should be able to suppress the noise included in the skeletons.

In order to suppress the noise impact present in the K-means method, a global thresholding is used to convert the intensity image into a binary image; then, the bright region(s) can be extracted from the background by a threshold value T. The following threshold value T obtained by preliminary experimental studies, is adopted to extract (a)

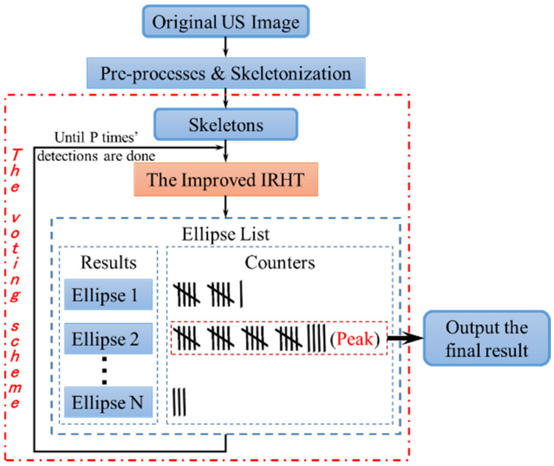

Fig. 1 Overview of the proposed method

bright region(s),

$$T = \mu_b - 0.75 \times \sigma_b \tag{1}$$

where μ_b is the mean value of the bright region, σ_b is the standard deviation of the bright region (Here, we suppose the bright region is classified into b-th cluster). In Eq. (1), "0.75" is the threshold for extracting only bones from three classes (bone, soft tissue, background). In addition, it is experimentally determined by our previous work[9].

As for binary image, a binary morphologic opening operation with a 2×2 window is used to remove some small bright regions. Morphologic dilation with a 1×1 window and closure with a 2×2 window are used to smooth the boundaries of the large bright regions. After the pre-processing, the skeletons of the bright region are extracted by distance transform[13].

Figure 2 (a)~(g) shows examples of the procedure of the pre-processing and skeletonization in US images. In which (a) :original fetal US image, (b): result of applying a bilateral filter to image (a), (c): result of applying a white top-hat transform to image (b), (d): segmentation result of applying the K-means clustering method to image (c), (e): result of applying a global thresholding with a threshold value T defined in Eq. (1) to image (d), (f): skeletons of the bright region extracted by applying distance transform to image (e), and (g): the original image is superimposed by the detection result for image(f), are shown based on the description in sections 2.3 and 2.4.

2.3 Improved iterative randomized Hough transform

In US images, fetal head skulls often appear as the bright region with some discontinuities, because fetal head skulls are not completely closed. In addition, some other structures

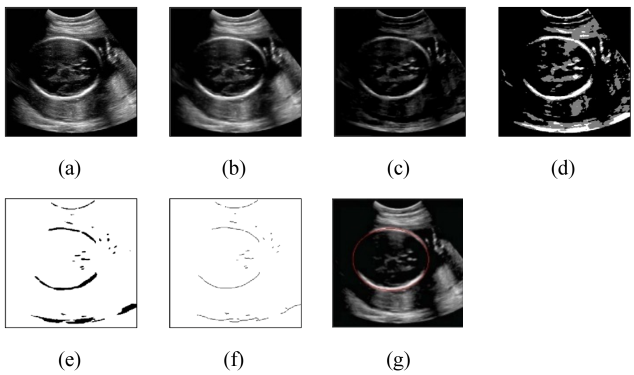

Fig. 2 Examples of the results by pre-processes and skeletonization

also may generate bright spots in US images. Furthermore, various artifacts and noise are usually present in US images. Accordingly, a useful head detection algorithm must effectively deal with these problems. To solve these problems, the authors developed an improved IRHT method[9] for detecting ellipses in US images despite the large discontinuities and strong noise for achieving more robust and accurate results, where the improved IRHT method is based on the original IRHT method[6]. In the following, the original and improved IRHT algorithms are overviewed.

2.3.1 Iterative randomized Hough transform

In a binary image, the curve to be detected can be modeled by $f(c,z) = 0$, where $c = [\alpha_1, \ldots, \alpha_2]^t$ comprises n-dimensional parameters, $z = (x, y)$ represents the coordinates of pixels on the curve. The RHT method[4] first randomly takes a sample of n pixels, $z_i = (x_i, y_i), i = 1, \ldots, n$, and maps this sample into one point $c \in R^n$ in the n-D parameter space by solving a set of n-equations $f(c, z_i) = 0$. If c is valid for (fits to) an ellipse, the counter at c is increased by one in the parameter space and stored in its corresponding accumulator. This process is repeated until a predefined number of valid samples (K) are processed. The location of the counter peak in the accumulators is outputted as the final detection result. For ellipse detection ($n = 5$), the following equation is utilized[13, 14] :

$$\mathrm{x}^2 + y^2 - U(x^2 - y^2) - V2xy - Rx - Sy - T = 0 \qquad (2)$$

where the five parameters, $[U, V, R, S, T]^t$, can be converted into the standard ellipse parameters $c = [x_0, y_0, a, b, \phi]^t$: (x_0, y_0) are the coordinates of the center of the ellipse, a and b are its major and minor semi-axes, and ϕ is the angle of rotation, then the ellipse eccentricity is given by $e = b/a$.

The IRHT method employs a randomized Hough transform (RHT) to a region of interest (ROI) in the image space by iterative parameter adjustment and reciprocal use of the image space and parameter space. The region of interest of RHT method is always the whole image, and it does not change during the whole process. However, the region of interest of the IRHT method is updated based on the latest estimates of the parameters during the iteration process, where the ROI is a little bit larger than the rectangle that circumscribes the latest ellipse. Note that IRHT tends to be trapped by non-fetal head, but ellipse-like objects, even if K is increased. Meanwhile, noise pixels are gradually excluded from the region of interest, and the estimation progressively gets accurate.

2.3.2 Improved iterative randomized Hough transform

On the basis of the principle of the IRHT method, we further introduce the number (N) of bright pixels on the detected ellipse as a goodness of the detected ellipse, because as shown in Fig. 2, the fetal head skull consists of many bright pixels In each iteration, K valid samples are detected by RHT method, and top-M peaks (Herein, M is experimentally selected to be ten) in the accumulators of the K valid samples are selected. Then, the number of pixels on the ellipse is calculated for the selected top-M peaks. Subsequently, the result with the maximal number of pixels on the ellipse is accepted as the result in each iteration, and used to update the region of interest for the next iteration. This iterative process continues until the size difference of the ROI between successive two iterations is very small, and the detected ellipse in the final iteration is the final result. Herein, the convergence conditions which is the same conditions used by IRHT method are: less than 2.5° in ϕ; less than 2 pixels in each of x_0, y_0, a and b; and less than 6 pixels total in x_0, y_0, a and b[9].

2.4 Voting scheme

As shown in **Fig. 3**, the method proposed in this paper is based on the improved IRHT method. The original IRHT method uses random sampling of five points, but the random sampling does not always give accurate results. The improved IRHT method can make a better detection accuracy because of counting the number of pixels on the detected ellipse to reduce the impact of sparse noise pixels. However, it may fail when the skeleton image extracted from the input US image are occupied by some noise curves.

Nevertheless, the curves of fetal head skull should be the most dominant components of the skeleton images,

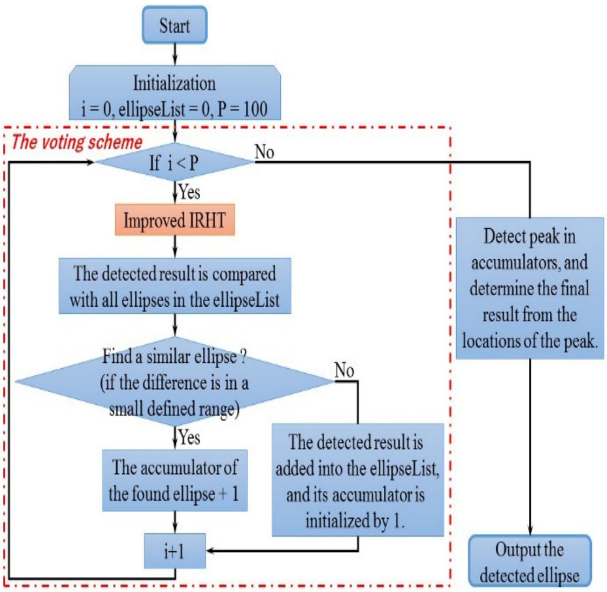

Fig. 3 Flow chart of the proposed method

compared with the noise curves. Thus, misdetection of the skull curves by the improved IRHT method should occur at a small probability. By considering these, multiple attempts by a voting scheme should be able to further reduce the probability of the misdetection.

Based on the results of P detections ($P = 100$ in this paper) by the improved IRHT method[9], the proposed method makes a list for saving all the detected results and their accumulators. For each detection, a voting is made for the results in the list. More specifically, the difference between the current detection result and each of the results saved in the list is compared: i.e., if the difference is within a pre-defined small range, then the accumulator of that result in the list is incremented by 1; otherwise, the current detection result is appended to the list as a new one. This process is repeated by P times. Consequently, the final result is determined by detecting the highest peak (with the most votes) in the accumulators from the list.

As mentioned earlier, Improved-IRHT reflects not only the count peaks in the accumulators (section 2.3.1) , but also the number of bright pixels; therefore, the ROI could be placed at different places in the image so that the fetal head can be detected at a high probability.

3. Experiments

US images containing fetal heads at about 20-32 weeks' gestational age are used for the experiments, where the US images are consolidated impossible anonymous. To heighten the performance of the algorithm, a priori information, reported by Hadlock et al. [2] is applied to the experiments: i.e., the eccentricity $e = b/a$ of the human fetal head has a mean (μ_e) of 0.783 and a standard deviation (σ_e) of 0.044. It could be used to construct a constraint as $\mu_e - 3\sigma_e \leq e \leq \mu_e + 3\sigma_e$, namely, $0.651 \leq e \leq 0.915$, and about 99.7% of fetal heads would have an eccentricity in this range. Therefore, only the result whose parameter e is within this range is accepted.

Although a strict convergence condition is used in the iterative process of the original and improved IRHT methods, as introduced in section 2.3.2, a relatively relaxed range is experimentally defined for the proposed voting scheme (the processing marked by a red doubly dotted line rectangle in Fig. 1) by less than 8.5° in ϕ; less than 5 pixels in each of x_0 and y_0; less than 6 pixels in each of a and b; and less than 19 pixels total in x_0, y_0, a and b. Namely, if the difference between the detected result and the ground truth made by experienced physicians is within such a relatively relaxed range, it is considered as a correct result; otherwise, it is a wrong result.

In addition, the program of ellipse detection is performed by a CPU E3-1240 v3 @ 3.40GHz. Since any optimization has not been considered currently, the efficiency of the algorithm could be able to be improved by 10-20 times based on parallel computation and GPGPU technology.

3.1 Experiment on the effect of noise

Two US images, each of which is contaminated by weak nose (**Fig. 4** (a): Image 1) and strong noise (Fig. 4 (b): Image 2), respectively, are used to evaluate the original IRHT method[6], the improved IRHT method (i-IRHT)[9] and the proposed method. The original images and the binary images of Image 1 and Image 2 are shown in Fig. 4. "Noise" in the images is sidelobes or artifact, which often occurs in ultrasound images. In addition, we make the pre-processing to reduce the noise such as the placenta of pregnant women in the images for the detection of the head of the fetus. Note that the binary image of Image 2 shown in Fig. 4 includes more noise than that of Image 1.

Each of the three methods is performed 50 times for each US image, and detection rate of each method in **Table 1** is obtained. The detection rate is calculated by the number of correct detection results divided by the total number of the detections (i.e., 50 times). Figure 4 shows the images used in Table 1.

In Table 1, a comparison of the results for the three methods is listed. We can observe that for Image 1 with weak noise, the three methods achieve high detection rates;

in particular, the proposed method achieves the best rate of 100%. However, for Image 2 with strong noise, only the proposed method can achieve a high detection rate of 92%, which is much higher than those of the other two methods. On the other hand, the result of the i-IRHT method is much better than that of the original IRHT method since the i-IRHT method considered the number of pixels on the ellipse. Consequently, the results in Table 1 indicate that the proposed method can achieve the best detection rate among the three methods, and a robust performance especially for images with strong noise. An example of the detection result is superimposed to the original image, as shown in Fig. 2 (g).

3.2 Experiment on different US images

30 US images (some examples are shown in **Fig. 5**, which have variations in terms of noise, the discontinuity and irregularity of fetal head skulls are used to evaluate the three methods, where each method is performed 50 times for each image.

In **Table 2**, the mean and standard deviation of the detection rates for the 30 US images are listed for each method. As written earlier, each of the three methods (IRHT, i-IRHT, Proposed method) is performed 50 times for each of the 30 US images (Table 2 etc.): that is, 1,500 performances by each method. The average in Table 2 shows the percentage (in 1,500 trials) of the correct detection. The standard deviation shows variations in the detection rate for each of the 30 US images. Table 2 demonstrates that the proposed method achieves much higher detection rate than the other two methods. It also indicates that the standard deviation of the detection rate by the proposed method is much smaller than the other two. This emphasizes that the proposed method is robust against wide variations in the noise, which are often contained in US images, such as, speckle noise, electronic noise and thermal noise. Although this method has a high detection rate, it is not 100%, so it may slightly detect erroneously. Also, since the conventional method can detect with accuracy as high as 70% or more,

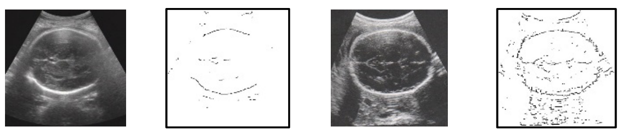

Image1(original) Image1(binary) Image2(original) Image2(binary)

(a) (b)

Fig.4 Images (original and binary) used in Table 1

Table 1 Detection rate of each method on two images

	IRHT	i-IRHT	Propose method
Image 1	88%	94%	100%
Image 2	30%	78%	92%

there is also the possibility of detecting an ellipse accurately than this method. However, as a point of view of this method, it can be cited as much as possible to reduce as much as possible about 30% of false detections occurring in the conventional method. It can be said that there are few cases where the accuracy of the conventional method is good by the proposed method which reduces the uncertainty due to acquisition of random points as much as possible.

The reason that the false case exists is that sometimes the detection accuracy of the conventional method IRHT is extremely low. Basically, the detection accuracy of IRHT is more than 70%, but some cases are close to 50%. Because the core of the i-IRHT and proposed methods are based on the conventional IRHT algorithm, the cases of extremely low detection accuracy by the conventional IRHT algorithm will result in false cases of the i-IRHT and proposed methods. On the other hand, the false case is very few for the i-IRHT and proposed methods based on the experiments.

3.3 Experiment on the number (N) of pixels on ellipse

As explained in section 2.3.2, since the proposed method and i-IRHT reflect the number of pixels on ellipses, **Table 3** compares the numbers of pixels on ellipses for different US images by IRHT, i-IRHT and the proposed method. Image 1 to Image 30 in Table 3 are ultrasonic images collected by us. Figure 5 (a) to (e) correspond to Image 4, Image 5, Image 1, Image 2, and Image 3, respectively. From Table 3, it can be seen that the number of pixels on ellipse by the i-IRHT algorithm are larger than those by the IRHT algorithm for each image.

(a) (b) (c) (d) (e)

Fig. 5 Some examples of the used 30 US images

Table 2 Mean and a standard d there is also the possibility of detecting an ellipse accurately

IRHT	i-IRHT	Proposed method
53.6%, 48.9%	76.5%, 30.36%	94.97%, 8.82%

Table 3 Comparison of the number of pixels *N* on ellipse

	IRHT	i-IRHT	Proposed method
Image 1	99	204	208
Image 2	90	205	203
Image 3	48	160	166
Image 4	96	158	156
Image 5	103	199	202
Image 6	24	189	191
Image 7	131	296	297
Image 8	130	210	214
Image 9	151	235	239
Image 10	67	194	189
Image 11	146	207	217
Image 12	95	150	155
Image 13	54	112	148
Image 14	98	153	165
Image 15	126	110	109
Image 16	152	270	269
Image 17	92	182	187
Image 18	37	166	169
Image 19	161	201	193
Image 20	101	157	159
Image 21	95	137	137
Image 22	103	227	232
Image 23	139	201	199
Image 24	136	226	244
Image 25	46	141	161
Image 26	87	139	158
Image 27	159	176	235
Image 28	102	197	182
Image 29	99	172	162
Image 30	82	122	121

(a) IRHT (b) i-IRHT

Fig. 6 Relationship between the skeleton image (black line) and the detected ellipse (red line)

Figure 6 is an illustration for evaluating the accuracy of the detection ellipse. The illustration in Fig. 6 meets the ellipse parameter condition (described from the fifth line of the second paragraph of section 3). It can be said that the fetal ellipse is detected accurately if number of pixels *N* on the ellipse is larger: i.e. i-IRHT's ellipse detection is more accurate.

The numbers of pixels *N* on the ellipse of the proposed method is similar to those of the i-IRHT algorithm, because the i-IRHT algorithm is iteratively carried out by our proposed method. Thus, considering the results shown in section 3.2, we can find that the accuracy of the proposed method is the best one compared with the IRHT and i-IRHT algorithms, as shown in Table 3.

3.4 Accuracy and efficiency

In section 2.4, for the voting scheme of the proposed method, *P*, the number of iterations is selected to be 100. In order to choose the best value of *P* for balancing the accuracy and efficiency, we conduct experiments for which *P* values change. The mean ellipse detection rates for different *P* values are shown in blue dots in Figure 6, in which *P* values are 10, 30, 50, 70, 80, 90, 100, 110, 120,130, 200, and 300.

As shown in orange dots in **Fig. 7**, the detection time increases with the increase in *P* value. On the other hand, the detection rate also increases with the increase in *P* value, but if *P* is larger than 110, the detection rate is not improved any more. Meanwhile, there is a case in which a high value locally exceeds the randomness included in the proposed method, because the detection rate deviates greatly at $P = 50$ (Fig. 7).

Concerning the computation costs for the proposed method and conventional IRHT, the proposed method's computation time increased linearly due to the triple loops for *P*, K and M, while the conventional method is linear to K. Therefore, the proposed method is worse in terms of the computational cost, but in practice, if the proposed method is implemented in CPU E3-1240 v3 @ 3.40GHz, the computation time is only several seconds.

Basically, the loop number *P* used by this method decides the accuracy of the ellipse detection, but actually the best detection rate of about 95% can be obtained when the *P* value is around 100.

On the other hand, images with low detection rates also exist. As shown in **Fig. 8** (a), sometimes accurate detection cannot be performed if the whole fetal head is not covered by the ultrasonic probe. This is because it is impossible to take the whole appearance of the ellipse and the tissue existing inside the ellipse is mis-detected as the head. Also, with regard to Fig. 8 (b), the lower right part of the ellipse is detected widely due to the problem of the incident angle of the probe. Therefore, when realizing the white top hat in the pre-processes, it is difficult to detect the correct ellipse, because important features are lost. In fact, when applying the proposed algorithm, it is assumed that the head region is accurately detected by the doctor; so we think that such cases can be tolerated for our application. Regarding Fig. 8 (c), it is possible to detect an ellipse exactly, but as far as we see, specific obtained parameters do not satisfy the above-mentioned conditions for the five parameters.

More specifically it does not satisfy the condition. Concerning ϕ, if the ellipse is close to a circle, ϕ tends to change drastically. In practice this is not a problem, but to evaluate the detection accuracy, we need to develop another condition.

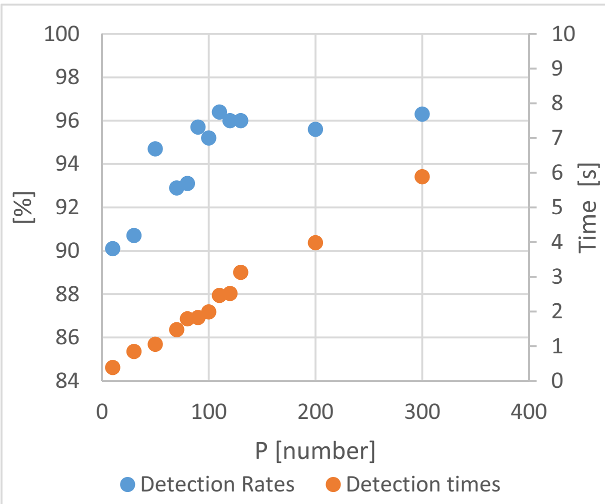

Fig. 7 Relationship between p values, accuracy (detection rate) and efficiency (detection time)

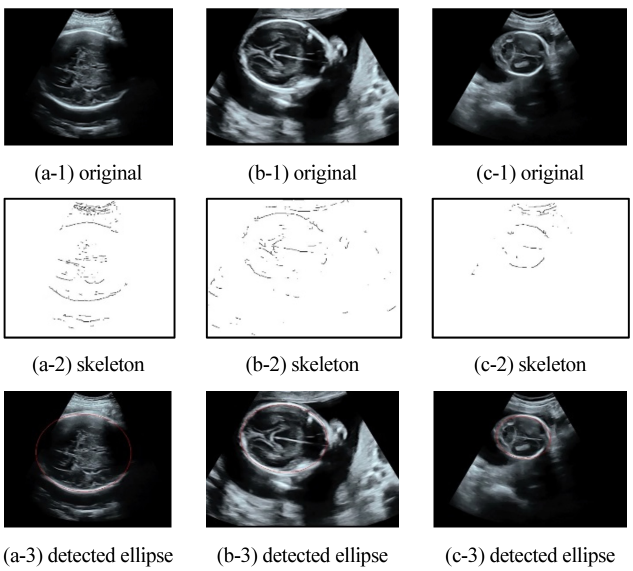

Fig. 8 Examples of difficult-to-detect images

3.5 Parameter evaluation in calculating the detection rate

In this section, it is assumed that the ellipse parameter condition is same as section 3.4. Although a certain number of ellipses can be accurately determined by this parameter, there are cases where accurate determination cannot be made for a small number of ellipses such as Fig. 8 (c). In order to accurately determine such an ellipse, it was also evaluated which parameters in the standard ellipse parameters $c = [x_0, y_0, a, b,]^t$ most affect. First, the mean squared error (MSE) of each parameter for P=100 by this method is calculated by Eq. (3).

$$\mathrm{MSE(c)} = \frac{1}{\mathrm{n}}\sum_{i=1}^{i}(x_i - c)^2 \qquad (3)$$

where c is the ground truth. The MSE calculation results for the five parameters are shown in **Table 4**.

From Table 4, it is found that the parameter that is most likely different from the ground truth is ϕ. The second is a, while the other parameters are not very different: that is, the detection accuracy of the center coordinates and the short axis are high. Artifact is the main reason why differences are prone to occur in the long axis a. In many cases, the outline of the bone is lost by artifact at both ends of the long axis of the fetal head ellipse. The angle ϕ is also affected by uncertainty due to the defective part of the major axis. In the future, we study how ϕ and a are adapted to different images.

Furthermore, we compare this method's average MSE with the conventional method (IRHT, i-IRHT). The average MSE of the standard ellipse parameters $c = [x_0, y_0, a, b, \phi]^t$ is calculated for each method and is shown in Table 5, where the average MSE is calculated as the average of the differences between the ground truth and estimation of each of the five ellipse parameters.

From **Table 5**, it is found that the proposed method gives the best MSE value of 3.853.

The case in which the proposed method's detection accuracy is worse than that of IRHT, though it is very rare, happens when IRHT's accuracy is very low. Since the proposed method is based on IRHT, the proposed method's accuracy is also low in such case. In contrast, when the proposed method's accuracy is very high, it is better than that of IRHT.

Table 4 Mean square error of the ellipse parameter

	a	b	x_0	y_0	ϕ
Image 1	7.43	0.78	5.73	0.74	18.49
Image 2	3.11	1.37	7.06	1.82	38.27
Image 3	2.14	0.36	2.94	0.69	11.89
Image 4	13.2	0.51	1.35	0.10	5.70
Image 5	2.07	1.83	1.21	0.66	2.04
Image 6	62.16	3.71	10.9	3.21	4.00
Image 7	11.64	8.29	8.38	4.38	11.43
Image 8	11.18	0.21	2.82	0.41	0.82
Image 9	4.91	0.61	2.37	1.25	5.62
Image 10	1.04	2.16	0.96	0.64	0.23
Image 11	36.83	1.19	21.2	3.33	6.60
Image 12	1.89	0.59	1.88	0.41	6.53
Image 13	4.51	0.67	2.17	0.17	1.80
Image 14	2.16	1.00	2.67	1.33	162
Image 15	3.67	26.45	2.64	25.17	24.44
Image 16	35.86	0.83	3.01	0.21	8.53
Image 17	4.84	0.64	0.98	0.16	0.84
Image 18	0.5	1.24	1.51	0.72	17.35
Image 19	2.86	2.29	1.04	1.25	20.3
Image 20	1.76	0.96	0,95	0.93	2.87
Image 21	8.53	9.83	5.01	7.73	8.44
Image 22	6.6	1.54	2.18	0.89	4.66
Image 23	12.7	1.27	3.01	1.23	61.80
Image 24	8.85	0.70	0.86	0.57	25.29
Image 25	1.44	9.83	5.01	7.73	8.44
Image 26	6.6	2.20	3.24	1.69	11.50
Image 27	7.35	0.99	4.82	0.55	13.42
Image 28	6.29	0.38	5.84	1.89	10.86
Image 29	10.01	0.59	1.88	0.41	6.53
Image 30	1.89	0.67	2.17	0.17	1.80

Table 5 Average MSE of each method

	IRHT	i-IRHT	Proposed method
Average	7.997	4.721	3.853

4. Conclusion

To achieve robust and accurate detection of fetal heads in US images, this paper has proposed a method that integrates an improved IRHT with a voting scheme. The proposed method votes the ellipse estimation result obtained by the improved IRHT to the parameter space and obtains the final detection result by finding the peak in the parameter space.

Experiments for comparing the proposed method with IRHT and improved IRHT using 30 US images demonstrate the effectiveness of the proposed method as follows.

- The proposed method can achieve much higher average detection rate (94.97%) and smaller standard deviation (8.82%).
- Larger numbers of fetal skull pixels on the detected ellipses are obtained by the proposed method than i-IRHT and IRHT.
- Ellipse detection rates for different loop numbers (*P*) of this method are explored. It turns out that 100 is the optimal value of *P* for the best detection rate.
- MSE for the five ellipse parameters obtained by the propose method are evaluated. The MSEs are reasonably small, but the ellipse rotation ϕ and the major axis *a* need further improvement.

Remaining issues include further improvement of the ellipse detection accuracy and efficiency by optimizing parameters used by the algorithm.

References

1) F. P. Hadlock, R.L. Deter, R. B. Harrist, S. K. Park: "Computer Assisted Analysis of Fetal Age in the Third Trimester Using Multiple Fetal Growth Parameters", Journal of Clinical Ultrasound, Vol. 11, pp. 313–316 (1983).
2) F. P. Hadlock, R. L. Deter, R. J. Carpenter, S. K. Oark : "Estimating Fetal Age: Effect of Head Shape on BPD", American Journal of Roentgenology, Vol. 137, No. 1, pp. 83–85 (1981).
3) I. Gull, G. Fait, J. Har-Toov, M. J. Kupferminc, J. B. Lessing, A. J. Jaffa, I. Wolma : "Prediction of Fetal Weight by Ultrasound: the Contribution of Additional Examiners", Ultrasound in Obstetrics and Gynecology, Vol. 20, No. 1, pp. 57–60 (2002).
4) L. Xu, E. Oja, P. Kultanen: "A New Curve Detection Method —Randomized Hough Transform (RHT)", Pattern Recognition Letters, Vol. 11, No. 5, pp. 331–338 (1990).
5) M. A. Fischler, R. C. Bolles: "Random Sample Consensus — A Paradigm for Model Fitting with Applications to Image Analysis and Automated Cartography", Communications of the ACM, Vol. 24, No. 6, pp. 381–395 (1981).
6) W. Lu, J. L. Tan: "Detection of Ellipse in Images with Strong Noise by Iterative Randomized Hough Transform (IRHT)", Pattern Recognition, Vol. 41, No. 4, pp. 1268–1279 (2008).
7) D. Ni, Y. Yang, S. Li, L. Shengli, Q. Jing, Q. Shuyuan, W. Tianfu, A.H. Pheng: "Learning Based Automatic Head Detection and Measurement from Fetal Ultrasound Images via

Prior Knowledge and Imaging Parameters", Proc. of International Symposium on Biomedical Imaging (ISBI), pp. 772–775 (2013).

8) S. Nie, J. Yu, P. Chen, J. Zhang, Y. Wang: "A Novel Method with a Deep Network and Directional Edges for Automatic Detection of a Fetal Head", Proc. of European Signal Processing Conference (EUSIPCO), pp. 654–658 (2015).

9) R. Xu, J. Ohya, B. Zhang Y. Sato, M. G. Fujie: "Automatic Fetal Head Detection on Ultrasound Images by an Improved Iterative Randomized Hough Transform", Automatic Fetal Head Detection on Ultrasound Images by an Improved Iterative Randomized Hough Transform", Proc. of Image and Vision Computing New Zealand (IVCNZ), pp. 288–292 (2011).

10) L. Breiman: "Bagging Predictors", Mach Learn, Vol. 24, No. 2, pp.123–140 (1996).

11) C. Tomasi, R. Manduchi: "Bilateral Filtering for Gray and Color Images", Proc. of the 1998 IEEE 6th International Conference on Computer Vision. pp. 839–846 (1998).

12) J. B. MacQueen: "Some Methods for Classification and Analysis of Multivariate Observations", Proc. of the fifth Berkeley symposium on mathematical statistics and probability, Vol. 1, pp. 281–297 (1967).

13) V. F. Leavers: "The Dynamic Generalized Hough Transform: Its Relationship to the Probabilistic Hough Transforms and an Application to the Concurrent Detection of Circles and Ellipses", CVGIP: Image Understanding, Vol. 56, No. 3, pp. 381–398 (1992).

14) A. B Forbes: "Fitting an Ellipse to Data", National Physical Laboratory Report DITC 95 (1987).

(Received August 12, 2017)
(Revised May 31, 2018)

Genta ISHIKAWA

He received B.S. degree from the Department of Modern Mechanical Engineering, the School of Creative Science and Engineering, Waseda University, Japan, in 2017. Currently, he belongs to the Department of Modern Mechanical Engineering, the Graduate School of the Creative Science and Engineering, Waseda University as an M.S. student. His research areas include deep learning, image processing, medical image processing and analysis, etc.

Rong XU

He received B.S. and M.S. degrees from the School of Information Science and Engineering and School of Computer Science and Engineering at China's Southeast University in 2003 and 2009, respectively. Also, he got Ph. D degree from Global Information and Telecommunication Studies at Waseda University in 2014. Currently, he works in a Japanese listed company, and his research and work are focused on deep learning on image processing, medical image processing and analysis, image-guided system, etc.

Jun OHYA (*Member*)

He earned B.S, M.S. and Ph.D. degrees in Precision Machinery Engineering from the University of Tokyo, Japan, in 1977, 1979 and 1988, respectively. He joined NTT Research Laboratories in 1979. NTT sent him to the University of Maryland, USA, for one year from 1988. He moved to ATR, Kyoto, Japan, in 1992. In 2000, he joined Waseda University as a professor. In 2005, he was a Guest Professor at the University of Karlsruhe, Germany. Since 2014, he has been a professor at the Department of Modern Mechanical Engineering, Waseda University. His research areas include computer vision and machine learning. Dr. Ohya is a member of IEEE, IIEEJ, IEICE, IPSJ and VRSJ.

Hiroyasu IWATA

He received the B.S., M.S., and Dr. of Engineering degrees in Mechanical Engineering from Waseda University in 1997, 1999, and 2003, respectively. He is currently a Professor, Department of Modern Mechanical Engineering, School of Creative Science and Engineering, Waseda University. He has published 140 papers. Since 2015, he has served as Director, Global Robot Academia Laboratory, Waseda University and appointed as a Next Generation Core Researcher in Key Researchers Development Program by Board of directors, Waseda University (since 2016) as well. His research interests include human assistive and augmentation robotics, skin adhesive bio-sensors, supernumerary robotic limb "Third Arm", echography-based prenatal checkup assistive robot, perception-assistive rehabilitation RT and artificial intelligence for construction machinery. He is a member of RSJ, JSME, SICE, EAJ and IEEE.